Thermal Decomposition and Mass Spectra of Phosphoramidate Esters

Choichiro SHIMASAKI,* Yoshinori MUTOU, Eiichi TSUKURIMICHI, and Toshiaki YOSHIMURA
Department of Industrial Chemistry, Faculty of Engineering, Toyama University, Gofuku, Toyama 930
(Received July 17, 1989)

Thermal decomposition of diphenyl phosphoramidate (**1**) and phenyl phosphordiamidate (**2**) was investigated by DTA-TG, IR, ^{1}H NMR, ^{31}P NMR, mass spectroscopy, and TG-GC/MS. The DTA-TG/DTG curve showed that the thermal decomposition of **1** occurred in one stage. Compound **1** melted at about 150 °C and decomposed to polyphosphates accompanied with a weight loss of about 60% in the temperature region of 200 to 350 °C. It was confirmed from the results of IR, ^{1}H NMR, and TG-GC/MS that this weight loss in TG of **1** is attributed to the liberation of ammonia and phenol and to the production of an insoluble polyphosphate through triphenyl phosphate or a soluble oligophosphate. The fragment ions of diphenyl ether (m/z 170) and aniline (m/z 93) were recognized in the mass spectrum of **1**. This result indicates that phenyl radical and hydrogen atom in both samples transfer between three oxygen atoms and a nitrogen atom around a phosphorus atom. The activation energy of the thermal decomposition was estimated to be 151 kJ mol^{-1} for **1** and 220 kJ mol^{-1} for **2**. From the DTA-TG/DTG curve of **2**, the decomposition in TG showed two stages and proceeded in a similar process to **1**. The cleavage of **2** by the electronic impact was also similar to that of **1**.

Some aryl phosphates[1] have been produced by the reaction of phenol with phosphoryl chloride in the presence of a tertiary amine. These phosphate esters have been investigated systematically as important intermediates of flame-proofing and fire-retardant agents. The present authors have reported on the thermal behavior of alkali (including ammonium) and alkaline earth salts of phosphoramidic acid.[2] This paper describes the thermal properties and the cleavage mechanism of **1** and **2** by the electronic impact.

Experimental

Preparation Methods. Commercial phenol and phosphoryl chloride were used without purification. Compounds **1** and **2** were prepared by adding phenol to phosphoryl chloride according to the method described in the literature.[3,4]

Measurements. Thermal analyses were carried out in air by a Rigaku Denki TG-DTA and DSC apparatus at various heating rates for TG-DTA and 5 °C min^{-1} for DSC, respectively. Calcinated alumina was used as the reference material. The TG-TRAP-GC/MS and TG-MS were carried out by a Shimadzu combined system in stationary helium gas at a heating rate of 10 °C min^{-1}. Elemental analysis was done by a Hitachi CHN Analyzer-026 at Toyama Medical and Pharmacy University. IR spectrum was recorded by a JASCO IR-810 for the KBr disc or thin film between rock salt plates. The ^{1}H, and ^{31}P NMR spectra of **1**, **2**, and the decomposition residue were measured in deuterated chloroform or/and dimethyl sulfoxide by a JNM-FX-90-FT-NMR instrument. TMS and orthophosphoric acid were used as the references. Mass spectra by the EI method were taken at ionization potential of 20 eV by a JEOL-JMS-D300.

Results and Discussion

Thermal Behavior. The DTA-TG curves of **1** and **2** are shown in Figs. 1 and 2 together with DTG. The DTA curve for **1** exhibited three endothermic peaks and an exothermic peak. The first peak (E_{D1} at 150.2 °C) is attributed to the melting of **1**. The second and third peaks (E_{D2} at 261.1 and E_{D3} at 276.5 °C) may be due to the intermediate stages for the condensation process, during which amine and phenyl groups are liberated to form triphenyl phosphate or polyphosphates. The final exothermic peak E_X over a wide temperature range of 310 to 400 °C is attributed to the condensation accompanied with the evolution of gas. The TG-DTG curve shows that the pyrolysis process for **1** takes place in three stages. In

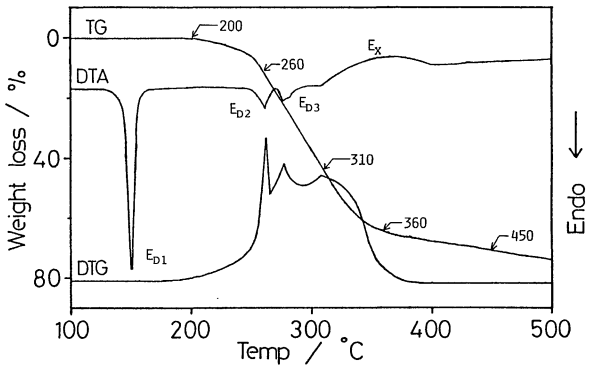

Fig. 1. Typical DTA-TG/DTG curves for **1**. Heating rate: 5 °C min^{-1}.

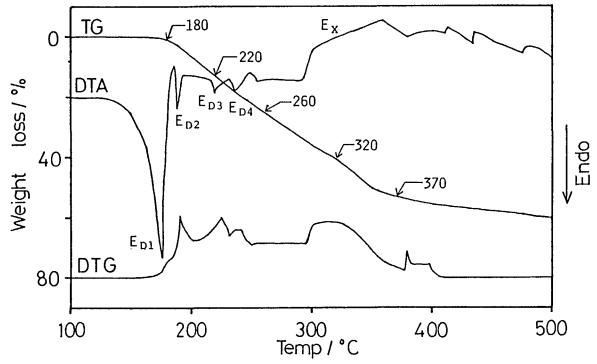

Fig. 2. Typical DTA-TG/DTG curves for **2**. Heating rate: 5 °C min^{-1}.

Fig. 1, the first peak of the DTG curve corresponds to the E_{D2} peak in the DTA curve for **1**, with the loss of water and ammonia, while the second and third peaks corresponding to the E_{D3} and E_X peaks may be the condensation to polyphosphates. In Fig. 2 the DTA curve for **2** exhibited four endothermic peaks and an exothermic peak. The first endothermic peak is attributed to the melting of **2**. The broad endothermic peaks after the melting of **2** indicate that water and ammonia are released slowly, leaving **1** or triphenyl phosphate behind. The final E_X peak for the formation of polyphosphates may be the same as that of **1**. The DTG curve shows that the pyrolysis of **2** takes place in complex stages. The above results were confirmed by TLC, IR, mass, and NMR spectra of **1** and **2** obtained before and after these endothermic peaks, as will be discussed later. The kinetic analysis was carried out on this thermal decomposition process according to Ozawa's method.[5] The TG curves obtained at the heating rates of 1, 5, 7, and 10 °C min^{-1} in air are depicted in Fig. 3a, in which the residual weight is plotted against the reciprocal of absolute temperature. In Fig. 3b is shown the Ozawa's plot of the logarithmic heating rate versus the reciprocal absolute temperature. The plot should yield a straight line, the slope of which gives the activation energy. The activation energy of the thermal decomposition calculated by the numerical least-squares fitting on a microcomputer was 151 and 220 kJ mol^{-1} for **1** and **2**, respectively.

Reaction Mechanism for Thermal Decomposition in Solid State. At the temperatures indicated on the TG curves in Figs. 1 and 2, the specimens were taken out from the furnace of DTA-TG, cooled in a silica gel desiccator, and subjected to further measurements. To confirm the changes in the TG curves as described in the previous section, IR, ^{1}H NMR, and ^{31}P NMR measurements were performed. Four spots were noticed on the thin-layer chromatogram oxidized with

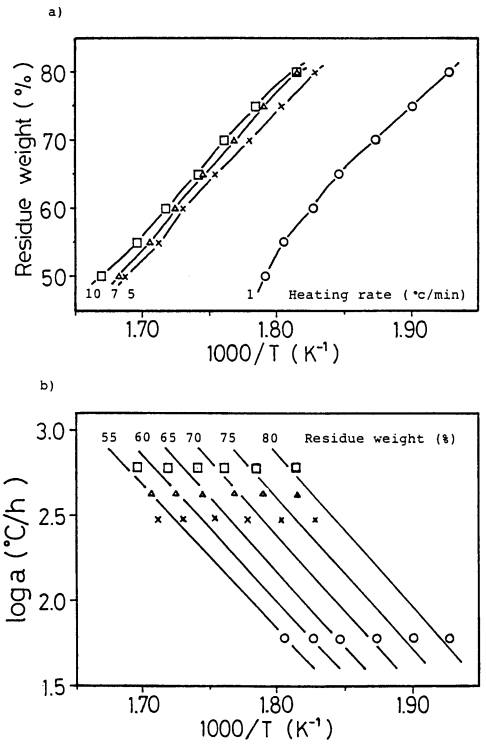

Fig. 3. Ozawa's plots.
a) TG curves of **1** plotted against reciprocal of absolute temperature.
b) Plots of logarithmic heating rate vs. the reciprocal absolute temperature for given inversion of decomposition of **1**.

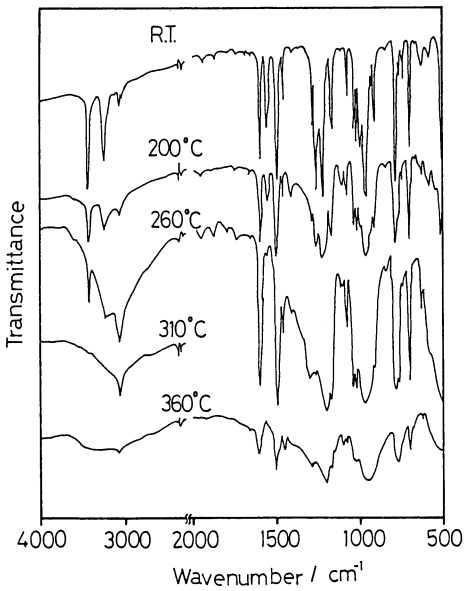

Fig. 4. IR spectra of the thermal decomposition products of **1**.
KBr method for R.T. and 360 °C; capillary film between rock salt plates for 200, 260, and 310 °C.

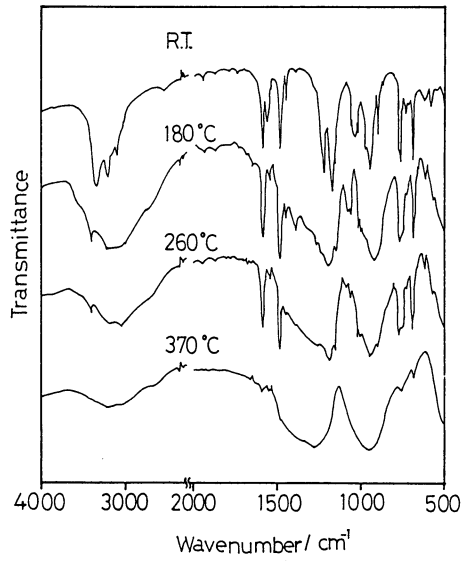

Fig. 5. IR spectra of the thermal decomposition products of **2** by KBr method.

iodine vapor for the residue at the 45% weight loss corresponding to 310 °C on the TG curve for **1**. It was attempted to isolate the four spots by column chromatography on silica gel to identify the constitution. The higher two spots were clearly separated and spectroscopically identified as triphenyl phosphate and **1**, respectively.

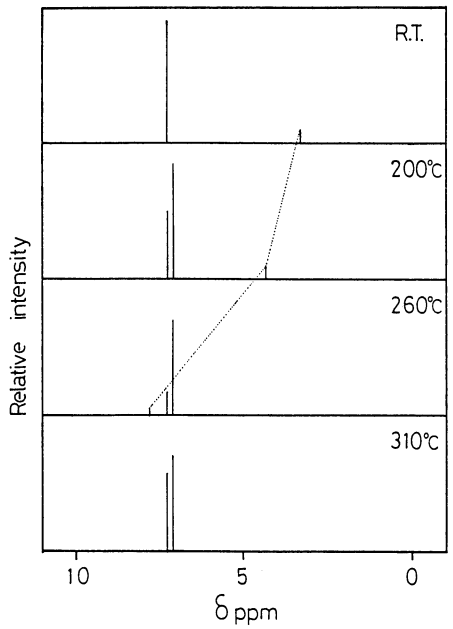

Fig. 6. ^{1}H NMR spectra of the thermal decomposition products of **1**.
Solvent: $CDCl_3$.

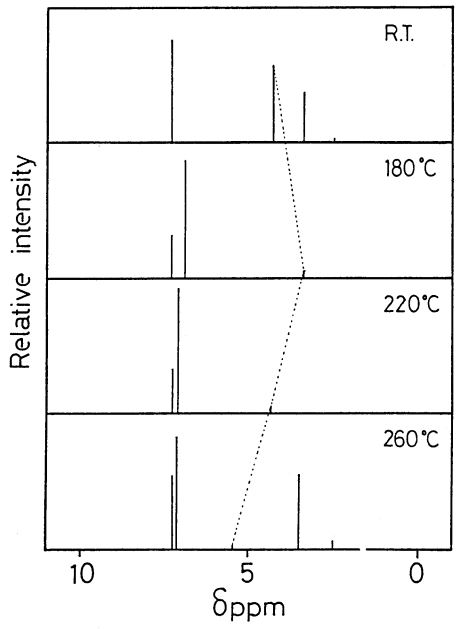

Fig. 7. ^{1}H NMR spectra of the thermal decomposition products of **2**.
Solvent: DMSO-d_6 for R.T. and 260 °C; $CDCl_3$ for 180 and 220 °C.

The IR spectra of the decomposition residues of **1** and **2** are shown in Figs. 4 and 5. In Fig. 4, the absorption band at 3425 cm^{-1} is assigned to the N-H stretching vibration; that at 1400 cm^{-1} to NH_4^+; that at 970—940 cm^{-1} to the P-O-P stretching vibration. The thermal decomposition of **1** at elevated temperatures proceeds through the formation of ammonium salt. The absorption of phenyl groups became stronger with increasing temperature and then disappeared, when direct P-O-P linkages seem to be formed. The above results suggest that triphenyl phosphate is formed as an intermediate. In the IR spectra of **2** in Fig. 5, the absorption bands for the amino and phenyl groups varied likewise during the progress of thermal decomposition and the decomposition mechanism of **2** may be explained similarly to that of **1**.

The ^{1}H NMR spectra of the decomposition residue of **1** and **2** are shown in Figs. 6 and 7, respectively. In the ^{1}H NMR spectrum of **1** before heating, the peak at about δ 7.3 is assigned to phenyl protons and that at δ 3.3 to amino protons. As the specimens were taken out at successively higher temperatures, the peak for phenyl protons splitted into two peaks, whereas amino protons became weaker with shifting to higher δ and then disappeared for the residue at 310 °C. In the ^{1}H NMR spectrum of **2** in Fig. 7, the peak at about δ 7.3 is assigned to phenyl protons, that at δ 4.3 to amino protons and that at δ 2.5 and 3.8 to the proton of solvent (DMSO-d_6). The peak for phenyl protons also splitted into two with increasing temperature, whereas the peak for amino protons became weaker with shifting to higher δ.

The ^{31}P NMR spectra of the residues of **1** are shown in Fig. 8. The ^{31}P NMR spectra of the residues at 200, 260, and 310 °C showed all or some of the peaks due to unknown material (phosphoramidate), **1**, orthophosphate, an endo-PO_4 group, and triphenyl phosphate. The peak which appeared at the highest magnetic field (at δ −17.5) was identified as triphenyl phosphate with reference to the standard sample which was prepared by an alternate procedure.[5]

The Fragmentation Mechanism of 1, 2, and Thermal Decomposition Products. The main cleavage mechanism of **1** and **2** is shown in Figs. 9 and 10. There are five cleavage patterns for both samples. The molecular ion peak for both samples was detected. The base peaks for **1** appeared at m/z 249(M^+) and for **2** at m/z 94 due to phenol. Two very characteristic peaks, the $(C_6H_5OH)^+$ at m/z 94 and $(C_6H_5NH_2)^+$ at m/z 93, appeared at both samples. These peaks were confirmed with the high resolution mass spectral data (Table 1) for the identification of atomic content of the ions. This table tabulates the exact mass of molecular ions, their elemental composition, the deviation of the theoretical mean values of the elemental composition from the observed mass in the high resolution mass spectral data, and the proba-

ble molecular structure of each identified component. From the fragment ion peaks at m/z 93 and 94, the groups such as phenyl radical and hydrogen atom seem to be eliminated easily by the electron impact. This result indicated that phenyl radical and hydrogen atom are transferred between oxygen and nitrogen atoms around a phosphorus atom. In addition, the peak due to the elimination of phenoxy radical (m/z 93) has also been detected. In **1**, the peak at m/z 170 is due to the fragment ion of diphenyl ether resulting from the loss of PO_2^+ and NH_2^+ from the molecular ion. The peak at m/z 66 is due to a fragment ion created by the loss of hydrogen cyanide from aniline and the loss of CO from phenol, although the peak height is low. The principal mass spectral data for compounds **1** and **2** heated at various temperatures are summarized in Table 2. In general, these spectra possess several common characteristics, particularly the presence of a large peak at m/z 326 (the molecular ion of triphenyl phosphate) and those at m/z 233 and 249. Each of these peaks were identified by the high resolution mass spectral data with triphenyl phosphates as authentic samples. It was thus confirmed that the thermal decomposition of **1** and **2** at elevated temperatures occurs through an intermediate such as triphenyl phosphate.

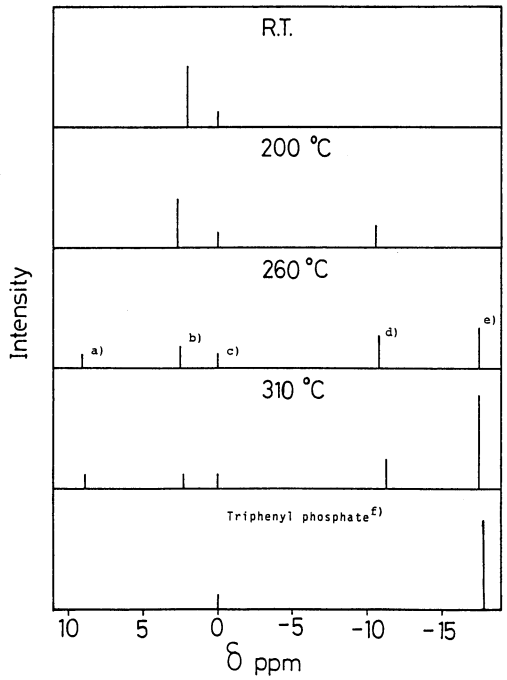

Fig. 8. ^{31}P NMR spectra of the thermal decomposition products of **1**.
a) Unknown material. b) Diphenyl amidophosphate. c) Orthophosphate. d) Endo-PO_4. e) Triphenyl phosphate. f) This standard sample was isolated by column chromatography using by silica gel.

Tandem Thermogravimetric Analyzer-Gas Chromatograph-Mass Spectrometer System. In order to investigate the thermal decomposition process of **1** and **2** showing DTA and TG curves described above over the range from 200 to 500 °C, TG-MS (Method-**A**) and TG-TRAP-GC/MS (Method-**B**) were carried out in stationary He gas. The effluent gas from TG was directly introduced into the mass spectrometer. In many cases, the TG effluent gas is composed of various components. Identification of less abundant components is more difficult. In addition, quantitative estimation of the constituents is more difficult. Another approach is to collect the pyrolysis products

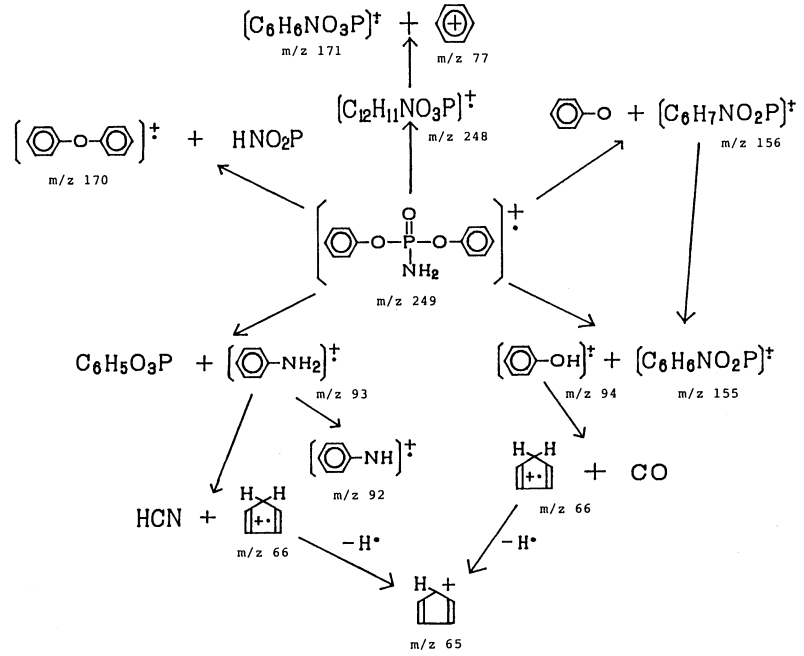

Fig. 9. Cleavage mechanism using by EI method for **1**.

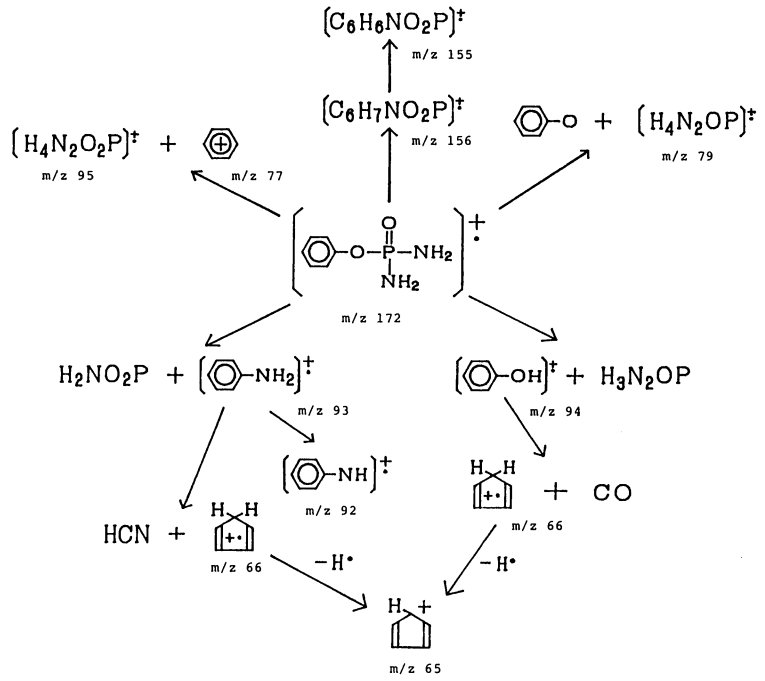

Fig. 10. Cleavage mechanism using by EI method for **2**.

Table 1. Mass Spectral Data for **1** and **2**

m/z	Relative intensity[a]	Sigma %	Observed molecular weight	U.S.[b]	Probable ion composition
(1) Diphenyl phosphoramidate (**1**)					
65	5.1	0.35	65.0382 (65.0390)[c]	3.5	C_5H_5
66	10.9	5.10	66.0433 (66.0468)	3.0	C_5H_6
77	503.8	11.35	77.0345 (77.0390)	4.5	C_6H_5
93	97.6	2.20	93.0539 (93.0576)	4.0	C_6H_7N
94	527.3	11.88	94.0408 (94.0417)	4.0	C_6H_6O
156	236.2	5.32	156.0102 (156.0211)	5.5	$C_6H_7NO_2P$
170	780.9	17.59	170.0733 (170.0729)	8.0	$C_{12}H_{10}O$
171	107.0	2.41	171.0052 (171.0082)	6.0	$C_6H_6NO_3P$
248	629.8	14.19	248.0383 (248.0472)	9.5	$C_{12}H_{11}NO_3P$
249	1000.0	22.53	249.0474 (249.0550)	9.0	$C_{12}H_{12}NO_3P$
(2) Phenyl phosphordiamidate (**2**)					
65	13.2	0.37	65.0471 (65.0390)	3.5	C_5H_5
66	52.4	1.49	66.0485 (66.0468)	3.0	C_5H_6
77	26.0	0.92	77.0371 (77.0390)	4.5	C_6H_5
79	370.2	13.10	79.0086 (79.0058)	1.5	H_4N_2OP
80	10.8	0.38	80.0254 (80.0136)	1.0	H_5N_2OP
93	447.3	15.83	93.0588 (93.0576)	4.0	C_6H_7N
94	1000.0	35.39	94.0342 (94.0417)	4.0	C_6H_6O
155	138.1	4.89	155.0112 (155.0133)	6.0	$C_6H_6NO_2P$
156	11.7	0.41	156.0174 (156.0211)	6.0	$C_6H_7NO_2P$
172	495.7	17.54	172.0397 (172.0397)	5.0	$C_6H_9N_2O_2P$

a) Relative intensity referred to base peak of spectrum as 1000. b) U.S.=Degree of unsaturation. c) Calculated values.

and analyze this collected material by GC. This method has been applied to the analysis of thermal degradation products of samples.[6-9] Figures 11 and 12 show TG curve and mass chromatogram of the liberated decomposition products of **1** and **2**, respectively, by Method-**A**. The thermally degraded products for both samples consist of a complex mixture of about five components: *m/z* 17, 18, 94, 249, and 326. In the case of **1**, these components were identified by measuring mass spectrum of the gas liberated from the principal portion of weight loss on the TG curve at 200 to 250 °C. Also, the peak at *m/z* 94 in the evolu-

Table 2. Mass Spectral Data of Decomposition Products for **1** and **2**

Temp/°C	*m/z*	Relative intensity[a]	Observed molecular weight	U.S.[b]	Probable ion composition
(1) Diphenyl phosphoramidate (**1**)					
200	249	1000.0	249.0610 (249.0550)[c]	9.0	$C_{12}H_{12}NO_3P$
	326	12.1	326.0428 (326.0703)	13.0	$C_{18}H_{15}O_4P$
310	233	146.0	233.0543 (233.0364)	9.5	$C_{12}H_{10}O_3P$
	249	43.8	249.0546 (249.0550)	9.0	$C_{12}H_{12}NO_3P$
	326	1000.0	326.0220 (326.0703)	13.0	$C_{18}H_{15}O_4P$
360	233	179.2	233.0312 (233.0364)	9.5	$C_{12}H_{10}O_3P$
	326	1000.0	326.0499 (326.0703)	13.0	$C_{18}H_{15}O_4P$
450	233	198.8	232.9887 (233.0364)	9.5	$C_{12}H_{10}O_3P$
	326	1000.0	326.0288 (326.0703)	13.0	$C_{18}H_{15}O_4P$
(2) Phenyl phosphordiamidate (**2**)					
180	249	832.5	249.0543 (249.0550)	9.0	$C_{12}H_{12}NO_3P$
220	249	907.5	249.0468 (249.0550)	9.0	$C_{12}H_{12}NO_3P$
	326	161.5	326.0701 (326.0703)	13.0	$C_{18}H_{15}O_4P$
260	233	125.3	233.0301 (233.0364)	9.5	$C_{12}H_{10}O_3P$
	249	549.8	249.0539 (249.0550)	9.0	$C_{12}H_{12}NO_3P$
	326	1000.0	326.0697 (326.0703)	13.0	$C_{18}H_{15}O_4P$
320	233	136.5	233.0408 (233.0364)	9.5	$C_{12}H_{10}O_3P$
	326	1000.0	326.0699 (326.0703)	13.0	$C_{18}H_{15}O_4P$

a) Relative intensity referred to base peak of spectrum as 1000. b) U.S.=Degree of unsaturation. c) Calculated values.

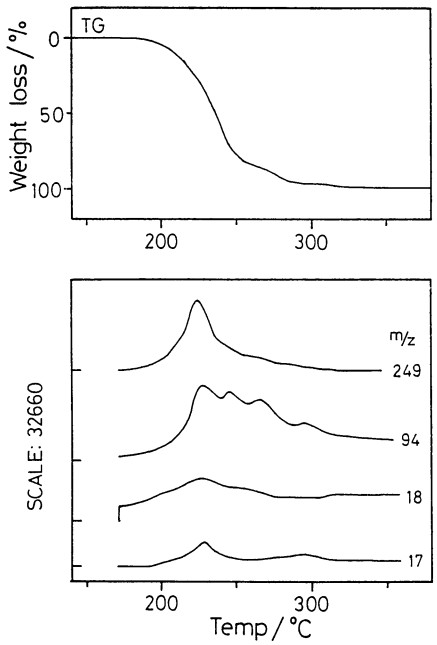

Fig. 11. TG curve and mass chromatogram of the evolved gas products by Method-**A** for **1**. Heating rate: 10 °C min^{-1}.

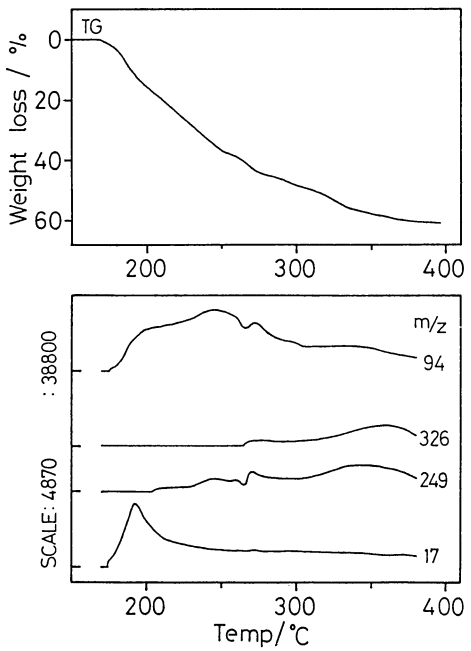

Fig. 12. TG curve and mass chromatogram of the evolved gas products by Method-**A** for **2**. Heating rate: 10 °C min^{-1}.

tion gas was detected throughout the thermal process. For sample **2**, on the other hand, the peak at *m/z* 17 only appeared clearly in the evolution gas of the initial portion of the TG curve, but other peaks were not completely elucidated in the thermal process. The peak at *m/z* 94 was finally appeared in a similar manner to **1**. Also, from the fragment ion peaks at *m/z* 249 and 326 for both samples, the groups such as phenyl seem to be eliminated easily and to travel around oxygen or nitrogen atoms on phosphorus atom. Figures 13 and 14 show the gas chromatogram of thermal decomposition products of **1** and **2** obtained by Method-**B**. The thermal decomposition products consist of a mixture of six components for **1**, and five components for **2**. When the Method-**B** was measured, the fragment ion peaks at *m/z* 249 and 326 were not observed. It is probable that the above fragment ions decompose on a column of porous

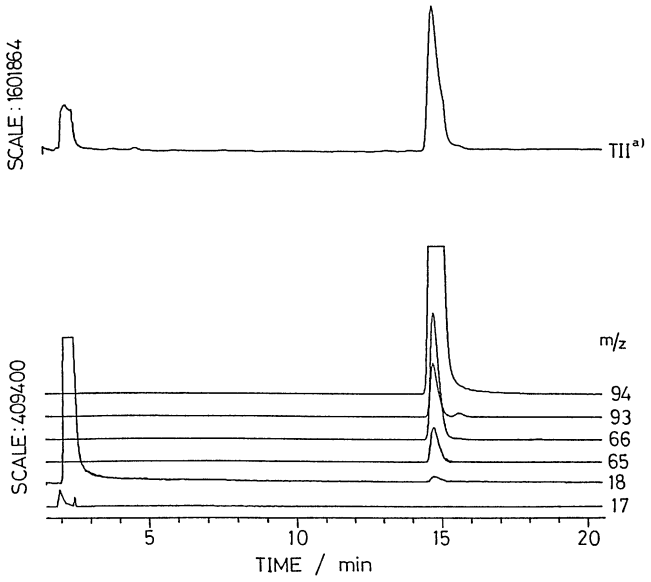

Fig. 13. Gas chromatogram of the evolved gas products by Method-**B** for **1**.
a) TII=Total Ion Intensity.

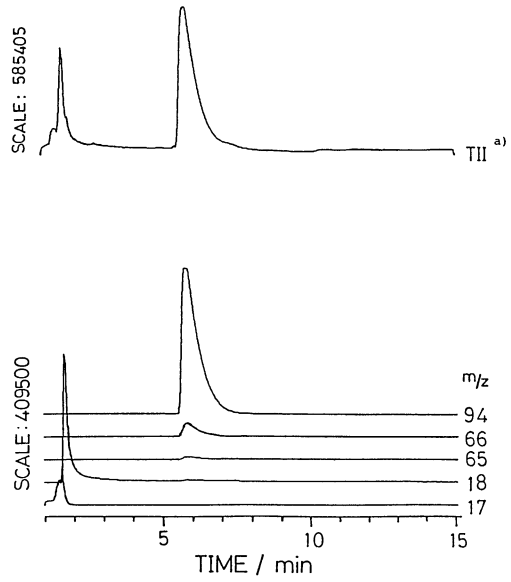

Fig. 14. Gas chromatogram of the evolved gas products by Method-**B** for **2**.
a) TII=Total Ion Intensity.

polymer beads of poly[oxy(2,6-diphenyl-1,4-phenylene)](TENAX GC).

According to these results, the following reaction processes can be written for the thermal decomposition of **1**. The following equations from Eqs. 1 to 5 describe some typical reaction schema.

(a) Decomposition

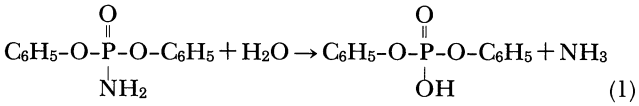

(1)

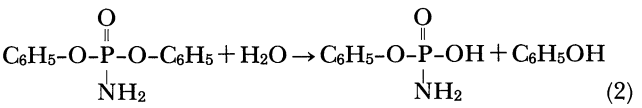

(2)

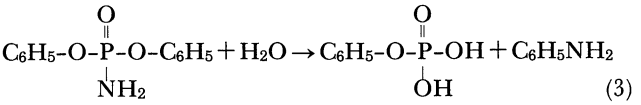

(3)

The water in the above reactions can come from adsorbed water on **1** and from a small amount of water in the reaction gas. Some reaction products in Eqs. 1, 2, and 3 were confirmed by direct comparison with authentic and commercial samples as references.

(b) Formation of intermediate substance

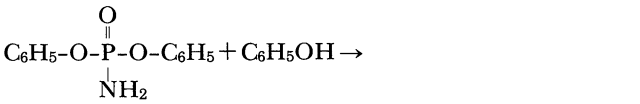

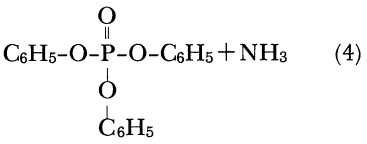

(4)

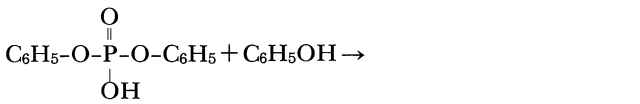

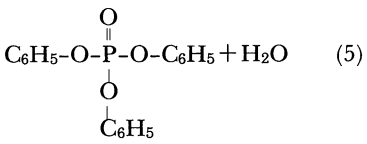

(5)

Together with the above reaction, a normal direct condensation was carried out. The corresponding reaction for **2** was finally carried out in a similar manner to the above. In the case of **2**, the formation of triphenyl phosphate occured at elevated temperatures through intermediate **1**.

The authors wish to thank for financial support by the Tamura Foundation for the Promotion of Science and Technology. The authors thank Miss Misao Shinoda for the mass spectra and Mr. Yoshiharu Yoneyama for NMR measurements.

References

1) J. R. Van Wazer, "Phosphorus and Its Compounds," Interscience Publishers Inc., New York (1961), Vol. II.

2) C. Shimasaki, Y. Oono, F. Takai, M. Shoji, and M. Yoshizawa, *Nippon Kagaku Kaishi*, **1982**, 376; C. Shimasaki, S. Ookawa, and R. Isizaka, *Bull. Chem. Soc. Jpn.*, **58**, 592 (1985); C. Shimasaki and M. Hara, *ibid.*, **58**, 3613 (1985); C. Shimasaki, H. Suzuki, and H. Toda, *ibid.*, **60**, 3050 (1987); C. Shimasaki and H. Suzuki, *ibid.*, **61**, 379 (1988).

3) R. Klement and K. H. Becht, *Zeit. Anorg. Allg. Chem.*, **254**, 217 (1947).

4) "Shin Jitsuken Kagaku Koza," ed by the Chemical Society of Japan, Maruzen, Tokyo (1976), Vol. 8, p. 354.
5) T. Ozawa, *Bull. Chem. Soc. Jpn.*, **38**, 1881 (1965); T. Ozawa, *J. Therm. Anal.* **2**, 301 (1962).
6) E. A. Boettner, G. Ball, and B. Weiss, *J. Appl. Polym. Sci.*, **13**, 377 (1969).
7) W. H. Hale, A. G. Farham, R. N. Johnson, and R. A. Clendiving, *J. Polym. Sci., Part A-1*, **5**, 2399 (1967).
8) J. Chiu, *Thermochim. Acta*, **1**, 231 (1970).
9) J. Chiu, *Anal. Chem.*, **40**, 1516 (1968).